

CHEMISTRY

A European Journal

A Journal of



Accepted Article

Title: COMPUTATIONAL NMR SPECTRA OF α -BENZYNE AND STABLE GUESTS AND THEIR HEMICARCEPLEXES

Authors: Abril Castro, Adrian Romero-Rivera, Sílvia Osuna, K.N. Houk, and Marcel Swart

This manuscript has been accepted after peer review and appears as an Accepted Article online prior to editing, proofing, and formal publication of the final Version of Record (VoR). This work is currently citable by using the Digital Object Identifier (DOI) given below. The VoR will be published online in Early View as soon as possible and may be different to this Accepted Article as a result of editing. Readers should obtain the VoR from the journal website shown below when it is published to ensure accuracy of information. The authors are responsible for the content of this Accepted Article.

To be cited as: *Chem. Eur. J.* 10.1002/chem.201904756

Link to VoR: <http://dx.doi.org/10.1002/chem.201904756>

Supported by
ACES

WILEY-VCH

Computational NMR Spectra of *o*-Benzyne and Stable Guests and their Hemicarceplexes

Abril C. Castro,^[a] Adrian Romero-Rivera,^[a] Sílvia Osuna,^[a,c] K. N. Houk,^[b] Marcel Swart^{*[a,c]}

[a] Dr. Abril C. Castro, Dr. Adrian Romero-Rivera, Prof. Sílvia Osuna, Prof. Marcel Swart*
Institut de Química Computacional i Catàlisi (IQCC), Departament de Química, Universitat de Girona
Campus de Montilivi, 17071 Girona, Spain.
E-mail: marcel.swart@gmail.com

[b] Prof. K. N. Houk
Department of Chemistry and Biochemistry, University of California
Los Angeles, CA 90095-1569, USA.

[c] Prof. Sílvia Osuna, Prof. Marcel Swart*
ICREA
Pg. Lluís Companys 23, 08010 Barcelona, Spain.

Supporting information for this article is given via a link at the end of the document.

Abstract: The incarceration of *o*-benzyne and 27 other guest molecules within hemicarcerand **1**, as reported experimentally by Warmuth, and Cram and co-workers, respectively, has been studied by density functional theory (DFT). ¹H-NMR chemical shifts, rotational mobility and conformational preference of the guests within the supramolecular cage were determined, which showed intriguing correlations of the chemical shifts with structural parameters of the host-guest system. Furthermore, based on the computed chemical shifts reassignments of some NMR signals are proposed. This affects in particular the putative characterization of the volatile benzyne molecule inside a hemicarcerand, for which our CCSD(T) and KT2 results indicate that the experimentally observed signals are most likely not resulting from an isolated *o*-benzyne within the supramolecular host. Instead, we show that the guest reacted with an aromatic ring of the host, and this adduct is responsible for the experimentally observed signals.

Introduction

One of the most exciting and challenging research fields in chemistry emerged in 1985 with Cram's synthesis of a molecule capable of trapping other molecules in its interior.^[1] Since then, the chemistry of molecular container compounds has become a challenging and rewarding field of organic chemistry.^[2-6] Early container molecules were shown to be able to encapsulate in their cavity almost any component present in the reaction mixture^[1] and were therefore called *carcerand* (from the Latin word *carcer*, *i.e.* prison). In these supramolecular hosts the encapsulated guest cannot leave the molecular *prison*, not even at high temperatures. In contrast, so-called *hemicarcerands* trap guests that can be liberated at elevated temperatures, with the combination of the host and guest called a hemicarceplex. The process of switching from encapsulation to liberation of the guest in these hemicarcerands was defined by Houk and co-workers as *gating*,^[5, 7-9] which involves a change in conformation of the supramolecular container molecule. Moreover, the (de)complexation processes are controlled by a process known as constrictive binding, which is related to the activation barrier required to trap the guest molecule inside the host cavity through a size-restricting portal.^[10] Several hemicarcerands have been synthesized by joining two

cavitands with several linkers^[3, 6] and a large variety of compounds have been incarcerated inside hemicarcerands cavities ranging from Xe^[10] to large molecules such as ferrocene, adamantane, camphor^[11] or C₆₀.^[12]

Nowadays, hemicarcerands and other classes of molecular containers can be used for many different applications in molecular recognition, catalysis, drug delivery, and storage.^[13-29] For instance, Cram and co-workers synthesized the highly reactive cyclobutadiene inside a hemicarcerand,^[30] and investigated the binding properties of hemicarcerands that can undergo chemical reactions without guest-release.^[31] In the literature, other examples have been given of unstable compounds that exhibit a high stability when encapsulated inside host molecules.^[3, 32-33] The finding that two benzene molecules perfectly fit into the cavity of some hemicarcerands, raised the idea of using the latter host molecules to perform bimolecular reactions.^[34] Kang and Rebek successfully performed a Diels-Alder reaction between *p*-benzoquinone and cyclohexadiene in a self-assembling molecular capsule,^[4] demonstrating that significant acceleration in the rates of chemical reactions may occur inside container molecules, just as was shown before inside cyclodextrins.^[35-36] In addition, a study by Piatnitski and Deshayes demonstrated that photochemical radiation is not only able to initiate reaction inside a hemicarceplex but it is also able to release guests from the host in a controlled manner when the host is designed to be susceptible to photolysis.^[37] Hence, the interior of a hemicarcerand has therefore been shown to be a suitable environment in which to synthesize and stabilize highly reactive compounds from thermal and photochemical reactions.

The *o*-benzyne molecule (see Figure 1), another vulnerable species that does not survive in solution or the gas phase, posed one of the most intriguing systems. Its existence was shown^[38] by NMR experiments on the photochemically generated *o*-benzyne molecule inside a molecular container. Soon after, the existence of *o*-benzyne was substantiated by low-level quantum chemistry calculations of the NMR spectra.^[39] More accurate calculations at coupled-cluster level^[40] and DFT level^[41] however showed significant deviations (*ca.* 1.0-1.5 ppm) from the experimental data, even though these methods usually give a much smaller deviation (*ca.* 0.3-0.5 ppm). The most likely origin for this difference is probably the fact that these calculations were done

FULL PAPER

on the isolated molecule, and not as a guest in the molecular container. However, given the high sensitivity of NMR, it cannot be completely discarded that the experimentally observed spectra do not belong to the *o*-benzyne molecule. Furthermore, benzyne was found to react with the hemicarcerand, so that NMR spectra attributed to benzyne are suspect.⁴³ It was also shown that the assignment of a molecular structure by experimental data alone can be tricky and may lead to wrong assumptions.⁴²

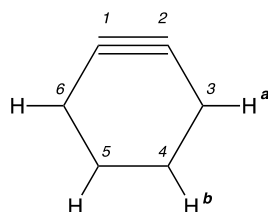


Figure 1. Structure of *o*-benzyne.

So far, the theoretical investigations of structures and dynamics of hemicarcerands have mainly involved force field (MM2, MM3, AMBER) and semiempirical calculations.^[9, 12, 43-48] While these methods calculate geometries and energies with sufficient accuracy to predict complexation behavior, it has been shown to have problems describing the unusual environment inside a hemicarcerand or hemicarceplex cavity accurately. This immediately suggests that more sophisticated methods are required on the full host-guest system to accurately analyze its electronic structure.^[49] Moreover, reports on the calculations of NMR parameters for hemicarceplexes are sparse, even though the ¹H-NMR spectroscopy has been proven to be a very valuable tool for determining the presence of guest inside a host and the stoichiometry of complexation. With this in mind, the overall aim of this work is to study computationally the structure and ¹H-NMR chemical shifts of hemicarcerand **1** (see Figure 2) and its corresponding hemicarceplexes with *o*-benzyne and a variety of 27 acyclic, cyclic or aromatic guests for which experimental data are available for comparison.^[38, 50] In particular, we have predicted the ¹H and ¹³C-NMR chemical shift constants of the isolated and incarcerated guests. Additionally, the rotational mobility and the conformational preference are described for the guest molecules.

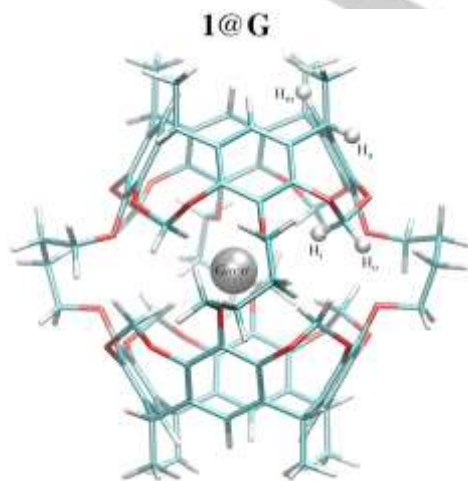


Figure 2. Hemicarcerand **1** with a guest **G** in its interior.

Results and Discussion

The well-known hemicarcerand **1** is globular-shaped and is composed by attaching two tetraaryl bowls to one another and their rims through four $-(\text{CH}_2)_4\text{O}-$ hemispheric bridges (see Figure 2). Likewise, four R groups ($\text{R} = \text{C}_6\text{H}_5\text{CH}_2\text{CH}_2$, $\text{CH}_3(\text{CH}_2)_4$) are attached to each bowl at their bases in **1**.^[50] X-ray structural determination has not been reported for empty **1**, and therefore our initial model system for the host is based on all the key features of the reported X-ray structures for the host-guest systems **1@G** (where **G** is any of $6\text{H}_2\text{O}$, $1,4\text{-I}_2\text{C}_6\text{H}_4$, *p*-xylene, $\text{C}_6\text{H}_5\text{NO}_2$, $(\text{CH}_3)_2\text{NCO}(\text{CH}_3)$ or $2\text{-BrC}_6\text{H}_4\text{OH}$).^[50] To reduce the computational effort, the R groups on the outside of **1** were replaced with methyl groups since they are expected to have a minor influence on the binding properties once the guest is inside. Indeed, the optimized structures at the PBE-D/TZ2P level of hemicarcerand **1** ($\text{R} = \text{C}_6\text{H}_5\text{CH}_2\text{CH}_2$, CH_3) showed that the effect of these groups on the core structure of the molecular container is negligible. Likewise, our model structure of host **1** ($\text{R} = \text{CH}_3$) presents a conformation where the methylene bridges $-(\text{CH}_2)_4-$ are all distributed on the outside of the container, and the upper hemisphere is twisted by 17° with respect to the lower hemisphere, which agree well with the twist angle of 15° reported for the X-ray structure of **1@6H₂O**.^[50] In contrast, a difference of 6° was found if compared with the optimized structure reported by Liddell and co-workers (twist of 23° , semiempirical AM1 method).^[49] The distance between the two oxygen atoms of each $-(\text{O}(\text{CH}_2)_4\text{O})-$ bridge varies between 2.80 and 2.82 Å and the separation between the two parallel square planes defined by the aryl carbons (bonded to H), used to define the length of the polar axis, is around 9.85 Å.

For the geometry optimizations of hemicarceplexes **1@G**, the guest molecules were introduced into the host starting from several initial host-guest geometrical configurations, placing the guests along the long polar and shorter equatorial axis of the host.

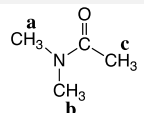
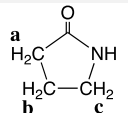
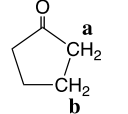
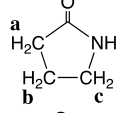
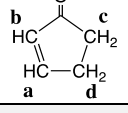
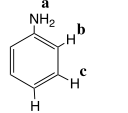
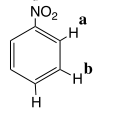
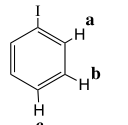
Guest molecules inclusion within host

First, we focus on the 28 different guest molecules that were incarcerated in the host **1**. Besides *o*-benzyne, the guest molecules can be divided into classes **A-F** regarding their shapes. Class **A** contains acyclic aliphatic compounds of three to six non-hydrogen atoms containing zero to two branches, class **B** includes five-membered ring compounds and classes **C-F** contain aromatic guests in which all the structures tend to be planar except for the methyl fragments of $1,4\text{-(CH}_3\text{O)}_2\text{C}_6\text{H}_4$ (**16d**) (see Figure S1).

The particular case of *o*-benzyne will be discussed separately. Hence, in the following we present the results for the other 27 guest molecules: Table 1 shows the calculated ¹H-NMR chemical shift values (δ) of the classes **A-F** guests, both on their own as well as when encapsulated inside host **1**; in it also are indicated the changes ($\Delta\delta$) that occur upon incarceration of the guests, and for comparison also the experimental values are included.^[50] In general, we found an excellent agreement between the calculated and experimental shift values, especially for the isolated molecules where 21 of the 27 guests show differences in chemical shifts of the order of ± 0.3 ppm or less in all their shifts (see $\Delta\delta$ of **G**, Table 1). On the other hand, only 7 of the 27 incarcerated guests (**1@G**) were found with similarly low $\Delta\delta$ values (see $\Delta\delta$ of **1@G**, Table 1). Accordingly, it appears that the host-guest interactions can alter the ¹H-NMR shift values dramatically and

FULL PAPER

Table 1. Calculated and experimental $^1\text{H-NMR}$ chemical shifts (δ) of free and incarcerated guests and their spectra changes in the chemical shifts of guest protons caused by incarceration ($\Delta\delta$).

Guest	Calculated			Experimental [‡]			Calc- Exptl		
	δ of G	δ of 1@G	$\Delta\delta$	δ of G	δ of 1@G	$\Delta\delta$	$\Delta\delta$ of G	$\Delta\delta$ of 1@G	$\Delta\Delta\delta$
Class A									
1a 	H _a , 2.94	H _a , -0.56	3.50	H _a , 3.02	H _a , -0.42	3.44	-0.08	-0.14	0.06
	H _b , 3.06	H _b , 1.71	1.35	H _b , 2.94	H _b , 1.61	1.33	0.12	0.10	0.02
	H _c , 2.04	H _c , -1.07	3.11	H _c , 2.08	H _c , -1.64	3.72	-0.04	0.57	-0.61
2a <chem>CH3CO2CH2CH3</chem>	H _a , 2.00	H _a , -2.18	4.18	H _a , 2.04	H _a , -2.19	4.23	-0.04	0.01	-0.05
	H _b , 4.28	H _b , 2.28	2.00	H _b , 4.11	H _b , 2.28	1.83	0.17	0.00	0.17
	H _c , 1.05	H _c , -1.47	2.52	H _c , 1.25	H _c , -1.97	3.22	-0.20	0.50	-0.70
3a <chem>CH3COCH3</chem>	H _a , 2.18	H _a , -0.83	3.00	H _a , 2.17	H _a , -0.83	3.00	0.01	0.00	0.00
4a <chem>CH3SOCH3</chem>	H _a , 2.38	H _a , -0.29	2.67	H _a , 2.46	H _a , -0.49	2.95	-0.08	0.20	-0.28
5a <chem>CH3CH2I</chem>	H _a , 1.87	H _a , -1.24	3.11	H _a , 1.84	H _a , -1.32	3.16	0.03	0.08	0.05
	H _b , 3.25	H _b , 1.66	1.59	H _b , 3.19	H _b , 1.35	1.84	0.06	0.30	-0.25
Class B									
6b 	H _a , 2.34	H _a , 0.90	1.44	H _a , 3.74	H _a , 0.50	3.24	-1.40	0.40	-1.80
	H _b , 2.17	H _b , 0.24	1.93	H _b , 2.89	H _b , 0.27	2.62	-0.72	-0.03	-0.69
	H _c , 4.32	H _c , 2.72	1.60	H _c , 5.35	H _c , 1.66	3.69	-1.03	1.06	-2.09
7b 	H _a , 2.09	H _a , -0.69	2.78	H _a , 2.15 [#]	H _a , 0.38	1.56	-0.06	-1.07	1.01
	H _b , 1.92	H _b , -0.15	2.07	H _b , 1.94 [#]	H _b , -0.31	2.46	-0.02	0.16	-0.18
8b 	H _a , 2.04	H _a , 0.36	1.68	H _a , 2.26	H _a , 0.26	2.00	-0.22	0.10	-0.32
	H _b , 2.09	H _b , -0.24	2.33	H _b , 2.12	H _b , -0.11	2.23	-0.03	-0.13	0.10
	H _c , 3.40	H _c , 1.98	1.42	H _c , 3.37	H _c , 0.69	2.68	0.03	1.29	-1.26
9b 	H _a , 8.12	H _a , 4.34	3.78	H _a , 7.70	H _a , 4.41	3.29	0.42	-0.07	0.49
	H _b , 6.15	H _b , 4.69	1.46	H _b , 6.17	H _b , 3.78	2.39	-0.02	0.91	-0.93
	H _c , 2.22	H _c , 1.49	0.73	H _c , 2.32 [#]	H _c , 0.51	2.16	-0.10	0.97	-1.07
	H _d , 2.85	H _d , -0.91	3.76	H _d , 2.67 [#]	H _d , 0.33	1.99	0.18	-1.24	1.42
Class C									
10c <chem>C6H6</chem>	H _a , 7.40	H _a , 5.13	2.27	H _a , 7.37	H _a , 4.70	2.67	0.03	0.43	-0.40
11c 	H _a , 3.71	H _a , -0.52	4.23	H _a , 3.64	H _a , -0.34	3.98	0.07	-0.18	0.25
	H _b , 6.63	H _b , 5.19	1.45	H _b , 6.69	H _b , 4.94	1.75	-0.06	0.24	-0.30
	H _c , 7.10	H _c , 5.13	1.98	H _c , 7.16	H _c , 5.36	1.80	-0.06	-0.24	0.18
	H _d , 6.60	H _d , 3.03	3.57	H _d , 6.76	H _d , 3.02	3.74	-0.16	0.01	-0.17
12c 	H _a , 8.38	H _a , 7.26	1.13	H _a , 8.23	H _a , 7.04	1.19	0.15	0.21	0.06
	H _b , 7.53	H _b , 5.69	1.85	H _b , 7.55	H _b , 5.90	1.65	-0.02	-0.22	0.19
	H _c , 7.70	H _c , 3.79	3.91	H _c , 7.70	H _c , 3.60	4.10	0.00	0.19	-0.19
13c 	H _a , 7.82	H _a , 6.68	1.15	H _a , 7.65	H _a , 6.65	1.00	0.17	0.03	0.15
	H _b , 7.08	H _b , 4.74	2.34	H _b , 7.40	H _b , 5.38	2.02	-0.32	-0.64	0.32
	H _c , 7.27	H _c , 3.33	3.94	H _c , 6.85	H _c , 3.32	3.53	0.41	0.01	0.40
Class D									
14d <chem>1,4-Br2C6H4</chem>	H _a , 7.27	H _a , 6.39	0.87	H _a , 7.29	H _a , 6.40	0.89	-0.02	-0.01	-0.01
15d <chem>1,4-(CH3)2C6H4</chem>	H _a , 2.29	H _a , -1.51	3.80	H _a , 2.32	H _a , -2.08	4.40	-0.03	0.57	-0.60
	H _b , 7.08	H _b , 5.78	1.30	H _b , 7.07	H _b , 5.90	1.17	0.01	-0.12	0.13
16d <chem>1,4-(CH3O)2C6H4</chem>	H _a , 3.76	H _a , 0.35	3.41	H _a , 3.77	H _a , -0.46	4.23	-0.01	0.81	-0.82
	H _b , 6.90	H _b , 5.69	1.21	H _b , 6.86	H _b , 5.82	1.04	0.04	-0.13	0.17
17d	H _a , 4.49	H _a , 8.29	-3.80	H _a , 7.91	H _a , 4.62	3.29	-3.42	3.67	-7.09

FULL PAPER

	a	b		H _b , 6.59	H _b , 6.06	0.53	H _b , 6.72	H _b , 5.27	1.45	-0.13	0.79	-0.92
	1,4-(OH)₂C₆H₄											
18d				H _a , 3.75	H _a , 0.32	3.43	H _a , 3.78	H _a , -0.35	4.13	-0.03	0.67	-0.70
				H _b , 6.80	H _b , 5.65	1.15	H _b , 6.81	H _b , 5.87	0.94	-0.01	-0.22	0.21
				H _c , 7.09	H _c , 5.64	1.45	H _c , 7.09	H _c , 5.87	1.22	0.00	-0.23	0.23
				H _d , 2.28	H _d , -2.29	4.57	H _d , 2.29	H _d , -2.11	4.40	-0.01	-0.18	0.17
19d				H _a , 6.89	H _a , 4.69	2.21	H _a , 6.81	H _a , 5.65	1.16	0.08	-0.97	1.05
				H _b , 7.20	H _b , 5.80	1.40	H _b , 7.00	H _b , 5.85	1.15	0.20	-0.05	0.25
				H _c , 2.32	H _c , -2.00	4.32	H _c , 2.23	H _c , -1.94	4.17	0.09	0.06	0.15
20d	1,4-I₂C₆H₄			H _a , 7.38	H _a , 6.92	0.47	H _a , 7.41	H _a , 6.73	0.68	-0.03	0.18	-0.22
Class E												
21e				H _a , 5.22	H _a , 4.04	1.18	H _a , 5.10	H _a , 4.00	1.10	0.12	0.04	0.08
				H _b , 6.79	H _b , 5.97	0.82	H _b , 6.85	H _b , 4.71	2.14	-0.06	1.26	-1.32
				H _c , 6.73	H _c , 3.17	3.56	H _c , 6.85	H _c , 4.39	2.46	-0.12	-1.22	1.10
22e				H _a , 2.30	H _a , -1.47	3.78	H _a , 2.28	H _a , -1.04	3.32	0.02	-0.43	0.46
				H _b , 7.07	H _b , 5.25	1.82	H _b , 6.95	H _b , 5.55	1.40	0.12	-0.30	0.42
				H _c , 6.97	H _c , 3.90	3.07	H _c , 6.95	H _c , 5.86	1.09	0.02	-1.97	1.99
				H _d , 7.11	H _d , 7.41	-0.30	H _d , 7.11	H _d , 5.80	1.31	0.00	1.61	-1.61
23e				H _a , 5.71 [#]	H _a , 6.13	0.07	H _a , 5.53	H _a , hidden	---	0.18	---	---
				H _b , 6.91 [#]	H _b , 2.29	4.71	H _b , 7.04 [#]	H _b , 6.30	1.17	-0.13	-4.01	3.88
				H _c , 7.13 [#]	H _c , 3.44	3.71	H _c , 7.24 [#]	H _c , 3.13	3.67	-0.11	-0.31	0.20
				H _d , 6.80 [#]	H _d , 5.72	1.07	H _d , 6.80 [#]	H _d , 6.21	1.03	0.00	-0.49	0.49
				H _e , 7.40 [#]	H _e , 6.18	1.21	H _e , 7.47 [#]	H _e , 3.77	3.27	-0.07	2.41	-2.48
Class F												
24f				H _a , 2.31	H _a , -1.21	3.51	H _a , 2.34	H _a , -1.47	3.81	-0.03	0.26	-0.30
				H _b , 7.21	H _b , 5.30	1.91	H _b , 7.35	H _b , 5.76	1.59	-0.14	-0.46	0.32
				H _c , 6.93	H _c , 6.59	0.34	H _c , 7.14	H _c , 5.47	1.67	-0.21	1.12	-1.33
				H _d , 7.19	H _d , 5.59	1.60	H _d , 7.14	H _d , 5.47	1.67	0.05	0.12	-0.07
25f				H _a , 2.18	H _a , 1.00	1.19	H _a , 2.21	H _a , -1.72	3.93	-0.03	2.72	-2.74
				H _b , 4.61	H _b , 0.07	4.54	H _b , 4.31	H _b , 4.67	-0.36	0.30	-4.60	4.90
				H _c , 6.60	H _c , 6.05	0.54	H _c , 6.64	H _c , 5.84	0.80	-0.05	0.21	-0.26
				H _d , 6.30	H _d , 5.33	0.97	H _d , 6.64	H _d , 5.84	0.80	-0.34	-0.51	0.17
				H _e , 4.34	H _e , 0.60	3.74	H _e , ---	H _e , ---	---	---	---	---
				H _f , 6.42	H _f , 3.96	2.46	H _f , 6.55	H _f , 5.78	0.77	-0.13	-1.82	1.69
26f				H _a , 2.28	H _a , -1.96	4.25	H _a , 2.31	H _a , -2.15	4.46	-0.03	0.19	-0.21
				H _b , 7.27	H _b , 5.37	1.90	H _b , 7.26	H _b , 5.76	1.50	0.01	-0.39	0.40
				H _c , 7.19	H _c , 6.35	0.84	H _c , 7.30	H _c , 6.77	0.53	-0.11	-0.42	0.31
				H _d , 6.90	H _d , 6.17	0.73	H _d , 7.00	H _d , 6.22	0.78	-0.10	-0.05	-0.05
27f				H _a , 2.22	H _a , -1.93	4.14	H _a , 2.24	H _a , -2.21	4.45	-0.02	0.28	-0.31
				H _b , 6.66	H _b , 5.29	1.37	H _b , 6.70	H _b , 5.25	1.45	-0.04	0.04	-0.08
				H _c , 5.53	H _c , 2.55	2.98	H _c , 5.10	H _c , 4.88	0.22	0.43	-2.33	2.76
				H _d , 4.64	H _d , 0.17	4.47	H _d , 4.95	H _d , 4.88	0.07	-0.31	-4.71	4.40
				H _e , 6.60	H _e , 5.77	0.83	H _e , 6.75	H _e , 6.21	0.54	-0.15	-0.44	0.29
				H _f , 6.47	H _f , 5.20	1.27	H _f , 6.61	H _f , 5.46	1.15	-0.14	-0.26	0.12

[#] Experimental values of reference **50**. [#] Values reassigned.

the orientation of the guest within host **1** might play a crucial role in some cases. Here, we report the results for the most favorable orientation of the guests inside the molecular container among the different possible orientations that we explored (see Supporting Information).

Typically, the chemical shifts of the encapsulated guests are 1-4 ppm shifted up-field, which likely depends on guest orientation and perhaps dynamics.^[51] The origin for this up-field shift is the magnetic shielding resulting from the benzene rings in the polar caps, and -OCH₂O- and -OCH₂Ar- groups, that form the

framework of the host. As a result, the ¹H-NMR shift values of class **A** (acyclic molecules) guests decrease upon complexation, ranging from $\Delta\delta = 1.35$ (for the H_b proton of (CH₃)₂NCOCH₃), to $\Delta\delta = 4.18$ ppm (for the H_a proton of CH₃COCH₂CH₃) (see Figure S1 for atom labeling). As expected from the parallel alignment of these guests along the main axis of the host, the chemical shifts of the terminal protons experience larger changes (larger $\Delta\delta$ values) than the internal protons. Examples are the terminal H_a and H_c protons of (CH₃)₂NCOCH₃ (**1a**), that have respective $\Delta\delta$ values of 3.50 and 3.11 ppm, whereas the H_b lies at 1.35 ppm.

FULL PAPER

Likewise, the $\text{CH}_3\text{CO}_2\text{CH}_2\text{CH}_3$ (**2a**) have $\Delta\delta$ values of 4.18 (H_a) and 2.52 ppm (H_c), whereas the internal H_b proton has a value of only 2.0 ppm (see $\Delta\delta$, Table 1).

Analysis of the $^1\text{H-NMR}$ signals of class **B** guests (five-membered ring structures) showed a different behavior. First, the large changes for the isolated 4-butyrolactone (**6b**) in experiment vs. theory, suggests strongly that in the experiment the isolated compound has either another conformation or another electronic structure. We ruled out an orientational effect, thus we varied the model geometry to another realistic structure, which is its protonated form (protonation of the carbonyl oxygen). Our results for the protonated guest show again the anticipated small differences between theory and experiment ($\Delta\delta$ values of ± 0.19 or less; see Table S1, SI), which suggests that in this case the protonated form is the one that was detected in the experiment. In the case of cyclopentanone (**7b**), our calculations clearly indicate an inversion of the assignment of the H_a and H_b spectral shifts. Thus, the experimentally observed peaks correspond to $\text{H}_a = 2.15$ and $\text{H}_b = 1.94$ ppm (isolated guest). A similar case was found for 2-cyclopenten-1-one (**9b**), where the H_c and H_d signals were also assigned inversely in the experimental study. Applying these changes to the experimental results, we obtained again small differences in the chemical shifts of the order of ± 0.42 ppm or less in all their shifts (see $\Delta\delta$ of **G**, Table 1).

The signal assignments of the class **B** incarcerated guests (**1@G**) turned out to be more complicated. The large $\Delta\delta$ values may indicate that in the experiment the guests have different conformation or electronic structure when encapsulated (see $\Delta\delta$ of **1@G**, Table 1). Similar to empty host **1**, these hemicarceplexes possess twisted conformations with angles that vary from 9° (**8b** and **10b** guests) to 16° (**9b** guest). Moreover, our molecular models, in conjunction with the large decrease of the chemical shifts caused by incarceration (see $\Delta\delta$, Table 1), suggest that these small guests may have strong interactions with the $-\text{O}(\text{CH}_2)_4\text{O}-$ bridges of the host. Furthermore, there exists the possibility that larger compounds, including disubstituted (classes **C**, **D** and **E**) and trisubstituted phenyl derivatives (class **F**), would remain in an extended form along the long polar axis of the host. In this study, the aromatic guests are aligned correctly inside the host (see Figure S2, SI), as reported in Reference 50. For example, a good agreement between the calculated and experimental twist angle was obtained for the $\text{C}_6\text{H}_5\text{NO}_2$ (**12c**) guest (0.8° difference between the optimized PBE-D/TZ2P structure and the reported X-ray structure). The class **D** compounds are the longest and most tightly held rigid guests. In particular, the cavity of the host **1** is spacious enough and complementary for the inclusion of 1,4- $(\text{CH}_3\text{O})_2\text{C}_6\text{H}_4$ (**15d**). The two $-\text{CH}_3\text{O}-$ groups of the guest nicely fit into the two hemispheres of the host, achieving stabilizing van der Waals interactions with the aromatic rings of the host. This is also consistent with the $^1\text{H-NMR}$ observations that the methyl protons certainly occupy the polar caps ($\Delta\delta = 3.80$) and whose Aryl-H atoms occupy the equatorial zone ($\Delta\delta = 1.30$) of the host.

It is well-known that phenol derivatives exhibit rotational isomerism.^[52] Hence, particular attention has been focused on the aromatic compounds with hydroxyl substituents: **17d**, **21e**, **23e**, **25f** and **27f** guests. No deviations from experiment were observed for the chemical shifts of the isolated **21e**, **25f**, and **27f** guests suggesting a strong preference to only one isomer. However, the **17d** and **23e** guests showed large discrepancies according to the experimental values (see $\Delta\delta$ of **G**, Table 1).

In 2-bromophenol (**23e**), there exist two isomers (*cis* and *trans*) originated from the orientation of the OH group with respect to the Br substituent (see Figure 3). Our results at the PBE-D/TZ2P corroborate the greater stability of the *cis* over the *trans* form, in agreement with the results reported in the literature.^[53] According to the calculations, these two forms are close in energy in gas phase ($\Delta E = 3.7$ kcal·mol⁻¹) and solvent, e.g. in chloroform solution using the COSMO model, has only a small effect on the energy gap ($\Delta E = 2.0$ kcal·mol⁻¹). Therefore, the populations of these two forms should be close or comparable and the consideration of only one form to calculate the chemical shifts may not be enough.

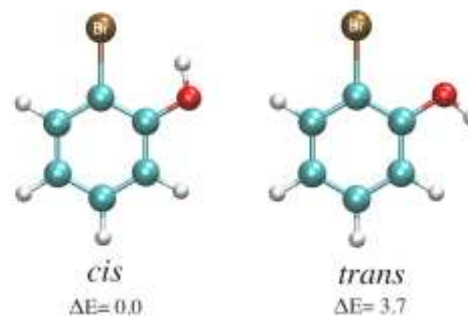


Figure 3. Structures of the *cis* and *trans* 2-bromophenol (**23e**) isomers. Relative energies are given in kcal·mol⁻¹.

The analysis of the $^1\text{H-NMR}$ shifts for the *cis* isomer of the 2-bromophenol (**23e**) shows that the calculated H_a proton value overestimates the experimental signal by 0.7 ppm. Further on, if to take into account that the calculation for the *trans* isomer predicts the H_a proton shift at higher field (underestimate the signal by -0.4 ppm), then the experimental value lies somewhere in between these two isomers which might be in fast exchange in the NMR time scale (see Table S2, SI). In the rest of the proton signals that form the aromatic ring, the calculations indicate that the two different pairs of signals, (H_b and H_e) and (H_c and H_d), were assigned inversely in the experimental study. Thus, applying these changes to the experimental results we obtained again small differences of the order of ± 0.18 ppm or less in all the chemical shifts (see $\Delta\delta$ of **G**, Table 1). Similar considerations can be applied for the incarcerated 2-bromophenol (**1@23e**), however, in this case the assignment of the signals becomes more difficult because the H_a peak is hidden in the experimental study. For benzene-1,4-diol (**17d**), the consideration of both *cis* and *trans* isomers does not help to reproduce the observed H_a shifts (see Table S2, SI). Therefore, we also explored solvent effects by adding two explicit water molecules that interact with the hydroxyl groups (see Table S1, SI). Interestingly, inclusion of the solvent molecules leads to a large deshielding of the H_a proton NMR signals; the obtained results are now in excellent agreement with experiment, with only 0.1 (H_a) and 0.2 (H_b) ppm difference. This finding indicates for **17d** the solvent effects play a larger role than the rotational isomerism.

Chemical shifts of incarcerated hosts **1@G**

Even though the guest signals are much more sensitive than the host signals to incarceration, the $^1\text{H-NMR}$ spectra of the hemicarceplexes themselves also might provide conclusive evidence for the incarceration of a guest within the container. The

FULL PAPER

host signals show sets of eight chemically different protons for the inward- (H_i) and outward-pointing acetal protons (H_o), the aryl protons (H_a), and the methine protons (H_m), of which we analyzed the H_i and H_o acetal protons that are the most sensitive to the presence of the guest (See Figure 2 for proton labels).

A comparison of the calculated and experimental H_i and H_o chemical shifts of free and incarcerated hosts **1@G** (δ), their chemical shift changes caused by incarceration ($\Delta\delta$), and the corresponding differences between these values are summarized in Table S3 of the Supporting Information. According to the experimental spectra,^[50] the H_i and H_o signals are equivalent when a symmetrical guest is encapsulated or when an unsymmetrical guest that is able to freely tumble inside the host in the $^1\text{H-NMR}$ time scale and makes the two halves of the host symmetrical. The important point to note is that for $\text{C}_6\text{H}_5\text{I}$ (**13c**), $4\text{-CH}_3\text{C}_6\text{H}_4\text{OCH}_3$ (**18d**), $2,4\text{-Cl}_2\text{C}_6\text{H}_3\text{CH}_3$ (**24f**), and $3,4\text{-Cl}_2\text{C}_6\text{H}_3\text{CH}_3$ (**26f**), the host signals (H_i and/or H_o) are split into two. This suggests that in the presence of the above guests the two halves of the host are not identical on the $^1\text{H-NMR}$ time scale. Thus, in these cases the inability of the guests to rotate around the short axis of the host causes the northern and southern hemispheres to be slightly different. This behavior was also identified in our calculations and, similar to the experimental signals, the deviations between the upper and lower hemispheres are of 0.3-0.5 ppm for the H_i shifts and 0.1-0.2 ppm for the H_o shifts (see δ , Table S3, SI).

If we compare our results and those reported by Cram and co-workers,^[50] we note a remarkable agreement between the calculated and experimental H_i and H_o shifts for the isolated host **1** and the incarcerated hosts **1@G**. The maximum deviations from the experimental values are of ± 0.6 or ± 0.5 ppm in the H_i and H_o shifts, respectively (see $\Delta\delta$, Table S3, SI). This reinforces the excellent agreement between experimental and theoretical determination of the $^1\text{H-NMR}$ chemical shifts of these hemicarcerands.

Encarceration of *o*-benzynes

In 1997, Warmuth made use of guest incarceration inside hemicarcerand **1** to stabilize the *o*-benzynes in solution.^[38] The $^1\text{H-NMR}$ spectra signals for incarcerated *o*-benzynes appear at 4.99 and 4.31 ppm. The first signal was assigned to H_a , and the latter to H_b . Stronger evidence for incarcerated *o*-benzynes was obtained from its $^{13}\text{C-NMR}$ spectrum. Three carbon signals for *o*-benzynes were found, as shown in Table 2. Additionally, an estimate for the chemical shifts of isolated *o*-benzynes in solution were obtained by taking the chemical shift differences $\Delta\delta$ (H) and $\Delta\delta$ (C) of incarcerated benzene as a measure for the host shielding and adding them to the observed chemical shifts of incarcerated *o*-benzynes (see experimental δ of **G**, Table 2).

In the case of the isolated *o*-benzynes, the calculated ^1H and $^{13}\text{C-NMR}$ shifts reported by Jiao and co-workers^[39] at the SOS-DFPT-PW91/III level are in reasonable agreement if compared with the data reported by Warmuth. However, discrepancies were found with the NMR calculations of Helgaker and co-workers, where the ^1H chemical shifts differ from the experimental values by more than is usual for such constants and the ordering of the observed protons is in inverse mode between theory ($H_a < H_b$) and experiment ($H_a > H_b$).^[54] It is important to note that all calculations reported until now were done on the isolated molecule. Computational studies for the *o*-benzynes as a guest inside a molecular container have not been reported yet.

With this in mind, we explored the incarceration of *o*-benzynes within hemicarcerand **1** (see Figures 1-2), starting from several initial host-guest geometrical configurations and placing the molecule along the long polar and shorter equatorial axes of the hosts. A stable conformation was achieved with the guest aligned along the long polar axis of the host (see Figure S3), in agreement with the minimum energy conformer reported by Cram and co-workers using molecular dynamics.^[45] At the KT2/ET pVQZ level, the $^1\text{H-NMR}$ shift constants obtained for the incarcerated *o*-benzynes are of 5.06 (H_a) and 5.33 ppm (H_b). If compared with the spectra signals reported by Warmuth,^[38] the calculated $^1\text{H-NMR}$ shift values are of 0.07 (H_a) and 1.02 ppm (H_b) larger than the experimental values (see $\Delta\delta$ of **1@G**, Table 2). Unlike experimental data, the host-guest (**1@G**) $^1\text{H-NMR}$ shifts indicate that H_a is more shielded than H_b .

The isolated *o*-benzynes have a "triple" bond length of 1.25 Å (at PBE-D/TZ2P) and 1.26 Å (at CCSD(T)/aug-cc-pVTZ), in good agreement with the bond length of 1.24 ± 0.02 Å obtained by Orendt and co-workers by a simulation of the ^{13}C dipolar NMR spectrum,^[55] and the bond length of 1.27 Å reported at the CCSD(T)/6-31G** level.^[56] A comparison of the NMR chemical shift results for the isolated *o*-benzynes molecule are shown in Table 2. Our $^1\text{H-NMR}$ chemical shift calculations obtained with both KT2/ET-pVQZ and CCSD(T)/pcS-3 methods, like those of Helgaker and co-workers,^[54] differ from the experimental values by more than is usual for such constants. At the KT2/ET-pVQZ level, the $^1\text{H-NMR}$ shift constants are of 6.77 (H_a) and 7.60 ppm (H_b). If compared with the experimental data reported by Warmuth,^[38] we found discrepancies of -0.92 and 0.59 ppm for the H_a and H_b protons, respectively (see $\Delta\delta$ of **G**, Table 2).

Interestingly, it is not only for the encapsulated *o*-benzynes that we find discrepancies, but also for the isolated form do we observe substantial differences. One should bear in mind that the experimental values of isolated *o*-benzynes were obtained by assuming the same large incarceration shift of 2.7 ppm for the two

Table 2. Comparison between the calculated and experimental ^1H and ^{13}C NMR chemical shifts in *o*-benzynes (ppm).

Nucleus	Calculated ^[a]			Experimental			Calc- Exptl		
	δ of G	δ of 1@G	$\Delta\delta$	δ of G	δ of 1@G	$\Delta\delta$	$\Delta\delta$ of G	$\Delta\delta$ of 1@G	$\Delta\Delta\delta$
H_a	6.77 (6.63) ^[b]	5.06	1.71	7.69	4.99	2.70	-0.92	0.07	-0.99
H_b	7.60 (7.53) ^[b]	5.33	2.27	7.01	4.31	2.70	0.59	1.02	-0.43
C1, C2	190.9 (195.5) ^[b]	190.9	0.02	182.7	181.3	1.38	8.20	9.55	-1.36
C3, C6	128.1 (128.6) ^[b]	126.4	1.69	126.9	125.5	1.41	1.21	0.93	0.28
C4, C5	140.8 (140.8) ^[b]	140.4	0.42	138.2	136.8	1.38	2.62	3.57	-0.96

[a] Computed at the PBE-D/TZ2P//KT2/ET-pVQZ level. [b] The shift values calculated using a geometry optimized at the CCSD(T)/aug-cc-pVTZ level are given in parentheses.

FULL PAPER

protons in *o*-benzyne, equal to the incarceration shift in benzene.^[38] Moreover, the conformational and dynamic effects may play an important role in this case. According to the dimensions of the guest and cavity of the host, the *o*-benzyne has space to move inside the host molecule and a static optimized geometry may not be enough for obtain accurate chemical shift values. Note also that the results can be complicated by the fact that *o*-benzyne can react with an aromatic ring of its hemicarcerand host.^[45, 57-61] For this reason, we examined the addition product of a Diels-Alder (DA) reaction between the *o*-benzyne and hemicarcerand **1**. *o*-Benzyne adds to one of the aryl ether units of **1** (diene component) to give the germinal para adduct (see Figure S4, SI). In the ¹H-NMR spectrum of the **1@o-benzyne** DA adduct, the proton signals originating from *o*-benzyne were identified at 6.14 (H_a), 5.21 (H_b), 4.58 (H_c), and 3.12 (H_d).^[61]

We optimized the **1@o-benzyne** DA adduct and calculated the ¹H-NMR chemical shifts. Interestingly, our results indicate an inversion of the assignment of the H_b and H_c spectral shifts. Thus, the experimentally observed peaks correspond to H_b= 4.58 and H_c= 5.21 ppm. Applying these changes, we found an excellent agreement between the calculated and experimental shift values, with small differences of the order of ±0.53 ppm or less in all their shifts (see Δδ of **G**, Table S4, SI).

Conclusion

In the present investigation, we have analyzed in detail the ¹H-NMR chemical shifts of the hemicarceplexes formed by *o*-benzyne and a variety of 27 guests within hemicarcerand **1** (**1@G**). Our study, via density functional theory (DFT) at the PBE-D/TZ2P level for geometries and KT2/ET-pVQZ level for the NMR shift constants, provides a new strategy to characterize these challenging host-guest complexes.

In the particular case of the *o*-benzyne guest, we obtained in both isolated and host-guest (**1@o-benzyne**) cases significant deviations from the ¹H-NMR experimental data and we cannot draw any definite conclusions regarding the assignment of the NMR chemical shifts. Surprisingly, we have shown that the discrepancies between theory and experiment are not due to the incarceration as asserted in earlier studies. The results shown here indicate that it cannot be conclusively determined whether the experimentally observed spectra belong to the *o*-benzyne molecule or to an adduct with an aromatic ring of the hemicarcerand. An investigation of the conformational and solvent effects combining molecular dynamic simulations and average NMR chemical shift calculations (similar to a recent study on a platinum complex^[62]) is currently underway for the incarcerated *o*-benzyne.

Computational Methods

All electronic-structure calculations of the isolated guests and the host-guest hemicarceplexes were performed using DFT. Equilibrium geometries were computed in the gas-phase with the Amsterdam Density Functional (ADF) program,^[63-64] using the QUILD program^[65] with the dispersion-corrected PBE-D^[66-67] functional in conjunction with uncontracted Slater-type orbitals (STOs) of triple-ζ quality plus one set of polarization functions (TZ2P).^[68] In particular for the guest structures that contain iodide atoms, scalar (SR) and spin-orbit (SO) relativistic effects

were included using the zeroth-order regular approximation (ZORA).^[69-73] Moreover, and additional optimization of the *o*-benzyne guest was computed at the CCSD(T)/aug-cc-pVTZ^[74-75] method with the CFOUR program.^[76-77]

All the ¹H and ¹³C-NMR chemical shift constants were calculated using the KT2 functional and the conductor-like screening model (COSMO)^[78-80] for simulating bulk solvation in chloroform. The ET-pVQZ all electron basis set was used for all atoms except iodine, for which we used the TZ2P basis set and the SR and SO relativistic effects were included using ZORA.^[69-73] All chemical shift values are reported with respect to tetramethylsilane (TMS) and were obtained with the GIAO method.^[81]

Supporting Information

Cartesian coordinates of all species will be made available at <http://iochem-bd.org>.

AUTHOR INFORMATION

Corresponding Author

* marcel.swart@gmail.com, @Marcel_Swart

ORCID identifiers

Abril C. Castro, 0000-0003-0328-1381
 Adrian Romero-Rivera, 0000-0002-0387-2774
 Sílvia Osuna, 0000-0003-3657-6469
 K.N. Houk, 0000-0002-8387-5261
 Marcel Swart, 0000-0002-8174-8488

Acknowledgements

The following organizations are thanked for financial support: MICINN (PhD-scholarship ACC CTQ2011-25086/BQU, projects CTQ2014-59212-P, CTQ2015-70851-ERC, CTQ2017-87392-P), CONACyT project 2014-383560, GenCat (PhD scholarship ARR 2015_FI_B_00165, 2014SGR1202 and XRQTC network) and European Fund for Regional Development (FEDER, UNGI10-4E-801).

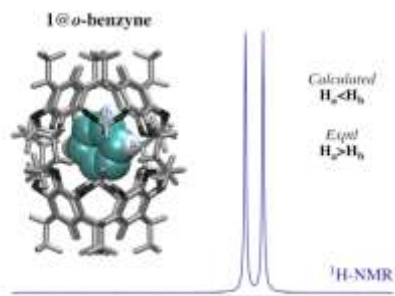
Keywords: Density functional calculations • Host-guest systems
 • NMR chemical shift calculations • *o*-benzyne

- [1] D. J. Cram, S. Karbach, Y. H. Kim, L. Baczynskyj, G. W. Kallemejn, *J. Am. Chem. Soc.* **1985**, *107*, 2575-2576.
- [2] Y. Liu, R. Warmuth, *Org. Lett.* **2007**, *9*, 2883-2886.
- [3] R. Warmuth, J. Yoon, *Acc. Chem. Res.* **2001**, *34*, 95-105.
- [4] J. Kang, J. Rebek, *Nature* **1997**, *385*, 50-52.
- [5] K. N. Houk, K. Nakamura, C. Sheu, A. E. Keating, *Science* **1996**, *273*, 627-629.
- [6] D. J. Cram, *Nature* **1992**, *356*, 29-36.
- [7] F. Liu, R. C. Helgeson, K. N. Houk, *Acc. Chem. Res.* **2014**, *47*, 2168-2176.
- [8] H. Wang, F. Liu, R. C. Helgeson, K. N. Houk, *Angew. Chem. Int. Ed.* **2013**, *52*, 655-659.
- [9] K. Nakamura, K. N. Houk, *J. Am. Chem. Soc.* **1995**, *117*, 1853-1854.
- [10] D. J. Cram, M. E. Tanner, C. B. Knobler, *J. Am. Chem. Soc.* **1991**, *113*, 7717-7727.
- [11] M. L. C. Quan, D. J. Cram, *J. Am. Chem. Soc.* **1991**, *113*, 2754-2755.

FULL PAPER

- [12] C. von dem Bussche-Hunnefeld, D. Buhning, C. B. Knobler, D. J. Cram, *J. Chem. Soc., Chem. Commun.* **1995**, 1085-1087.
- [13] D. Lozano, R. Álvarez-Yebra, R. López-Coll, A. Lledó, *Chem. Sci.* **2019**.
- [14] Y. V. Aulin, M. Liu, P. Piotrowiak, *J. Phys. Chem. Lett.* **2019**, *10*, 2434-2438.
- [15] M. A. Romero, P. Mateus, B. Matos, Á. Acuña, L. García-Río, J. F. Arteaga, U. Pischel, N. Basílio, *J. Org. Chem.* **2019**, *84*, 10852-10859.
- [16] D. Shimoyama, T. Haino, *J. Org. Chem.* **2019**.
- [17] J. Chyba, M. Novák, P. Munzarová, J. Novotný, R. Marek, *Inorg. Chem.* **2018**, *57*, 8735-8747.
- [18] A. Jaroš, Z. Badri, P. L. Bora, E. F. Bonab, R. Marek, M. Straka, C. Foroutan-Nejad, *Chem. Eur. J.* **2018**, *24*, 4245-4249.
- [19] C. Gropp, B. L. Quigley, F. Diederich, *J. Am. Chem. Soc.* **2018**, *140*, 2705-2717.
- [20] D. Zhang, A. Martinez, J.-P. Dutasta, *Chem. Rev.* **2017**, *117*, 4900-4942.
- [21] A. M. Raj, M. Porel, P. Mukherjee, X. Ma, R. Choudhury, E. Galoppini, P. Sen, V. Ramamurthy, *J. Phys. Chem. C* **2017**, *121*, 20205-20216.
- [22] A. Díaz-Moscoso, P. Ballester, *Chem. Commun.* **2017**, 53, 4635-4652.
- [23] C. Foroutan-Nejad, V. Andrushchenko, M. Straka, *Phys. Chem. Chem. Phys.* **2016**, *18*, 32673-32677.
- [24] K. Hermann, Y. Ruan, A. M. Hardin, C. M. Hadad, J. D. Badjić, *Chem. Soc. Rev.* **2015**, *44*, 500-514.
- [25] D. S. Kim, J. L. Sessler, *Chem. Soc. Rev.* **2015**, *44*, 532-546.
- [26] S. Zarra, D. M. Wood, D. A. Roberts, J. R. Nitschke, *Chem. Soc. Rev.* **2015**, *44*, 419-432.
- [27] L. Avram, Y. Cohen, *Chem. Soc. Rev.* **2015**, *44*, 586-602.
- [28] V. Ramamurthy, S. Jockusch, M. Porel, *Langmuir* **2015**, *31*, 5554-5570.
- [29] M.-J. Li, C.-H. Huang, C.-C. Lai, S.-H. Chiu, *Org. Lett.* **2012**, *14*, 6146-6149.
- [30] D. J. Cram, M. E. Tanner, R. Thomas, *Angew. Chem. Int. Ed.* **1991**, *30*, 1024-1027.
- [31] C. N. Eid, C. B. Knobler, D. A. Gronbeck, D. J. Cram, *J. Am. Chem. Soc.* **1994**, *116*, 8506-8515.
- [32] R. Warmuth, S. Makowiec, *J. Am. Chem. Soc.* **2005**, *127*, 1084-1085.
- [33] R. Warmuth, S. Makowiec, *J. Am. Chem. Soc.* **2007**, *129*, 1233-1241.
- [34] J. Kang, J. Rebek, *Nature* **1996**, *382*, 239-241.
- [35] N. K. Sangwan, H.-J. Schneider, *J. Chem. Soc., Perkin Trans. 2* **1989**, 1223-1227.
- [36] D. D. Sternbach, D. M. Rossana, *J. Am. Chem. Soc.* **1982**, *104*, 5853-5854.
- [37] E. L. Piatnitski, K. D. Deshayes, *Angew. Chem. Int. Ed.* **1998**, *37*, 970-972.
- [38] R. Warmuth, *Angew. Chem. Int. Ed.* **1997**, *36*, 1347-1350.
- [39] H. Jiao, P. v. R. Schleyer, R. Warmuth, K. N. Houk, B. R. Beno, *Angew. Chem. Int. Ed.* **1997**, *36*, 2761-2764.
- [40] T. Helgaker, M. Jaszuński, *J. Chem. Theory Comput.* **2006**, *3*, 86-94.
- [41] L. Armangué, M. Solà, M. Swart, *J. Phys. Chem. A* **2011**, *115*, 1250-1256.
- [42] S. Osuna, A. Rodríguez-Forteza, J. M. Poblet, M. Sola, M. Swart, *Chem. Commun.* **2012**, *48*, 2486-2488.
- [43] X. Wang, Z. Yang, J. Wang, J. Zhang, W. Cao, *J. Mol. Struct.: THEOCHEM* **2006**, *766*, 169-175.
- [44] R. Warmuth, J.-L. Kerdelhué, S. Sánchez Carrera, K. J. Langenwalter, N. Brown, *Angew. Chem. Int. Ed.* **2002**, *41*, 96-99.
- [45] B. R. Beno, C. Sheu, K. N. Houk, R. Warmuth, D. J. Cram, *Chem. Commun.* **1998**, 301-302.
- [46] K. Nakamura, C. Sheu, A. E. Keating, K. N. Houk, J. C. Sherman, R. G. Chapman, W. L. Jorgensen, *J. Am. Chem. Soc.* **1997**, *119*, 4321-4322.
- [47] C. Sheu, K. N. Houk, *J. Am. Chem. Soc.* **1996**, *118*, 8056-8070.
- [48] R. C. Helgeson, K. Paek, C. B. Knobler, E. F. Maverick, D. J. Cram, *J. Am. Chem. Soc.* **1996**, *118*, 5590-5604.
- [49] M. J. Liddell, D. Margetic, A. S. Mitchell, R. N. Warrener, *J. Comput. Chem.* **2004**, *25*, 542-557.
- [50] T. A. Robbins, C. B. Knobler, D. R. Bellew, D. J. Cram, *J. Am. Chem. Soc.* **1994**, *116*, 111-122.
- [51] D. J. Cram, M. T. Blanda, K. Paek, C. B. Knobler, *J. Am. Chem. Soc.* **1992**, *114*, 7765-7773.
- [52] T. Lin, E. Fishman, *Spectrochim. Acta A: Mol. Spectrosc.* **1967**, *23*, 491-500.
- [53] D. N. Shin, J. W. Hahn, K.-H. Jung, T.-K. Ha, *J. Raman Spectrosc.* **1998**, *29*, 245-249.
- [54] T. Helgaker, O. B. Lutnaes, M. Jaszuński, *J. Chem. Theory Comput.* **2007**, *3*, 86-94.
- [55] A. M. Orendt, J. C. Facelli, J. G. Radziszewski, W. J. Horton, D. M. Grant, J. Michl, *J. Am. Chem. Soc.* **1996**, *118*, 846-852.
- [56] E. Kraka, D. Cremer, *Chem. Phys. Lett.* **1993**, *216*, 333-340.
- [57] B. R. Reiner, I. A. Tonks, *Inorg. Chem.* **2019**, *58*, 10508-10515.
- [58] X. Xiao, T. R. Hoye, *J. Am. Chem. Soc.* **2019**, *141*, 9813-9818.
- [59] F. Hirsch, E. Reusch, P. Constantinidis, I. Fischer, S. Bakels, A. M. Rijs, P. Hemberger, *J. Phys. Chem. A* **2018**, *122*, 9563-9571.
- [60] J. Torres-Alacan, *J. Org. Chem.* **2016**, *81*, 1151-1156.
- [61] R. Warmuth, *Chem. Commun.* **1998**, 59-60.
- [62] A. C. Castro, H. Fliegl, M. Cascella, T. Helgaker, M. Repisky, S. Komorovsky, M. Á. Medrano, A. G. Quiroga, M. Swart, *Dalton Trans.* **2019**, *48*, 8076-8083.
- [63] G. te Velde, F. M. Bickelhaupt, E. J. Baerends, C. Fonseca Guerra, S. J. A. van Gisbergen, J. G. Snijders, T. Ziegler, *J. Comput. Chem.* **2001**, *22*, 931-967.
- [64] E. J. Baerends, and co-workers, *ADF2014.01, SCM, Theoretical Chemistry, Vrije Universiteit, Amsterdam, The Netherlands, http://www.scm.com/*.
- [65] M. Swart, F. M. Bickelhaupt, *J. Comput. Chem.* **2008**, *29*, 724-734.
- [66] S. Grimme, *J. Comput. Chem.* **2006**, *27*, 1787-1799.
- [67] J. P. Perdew, K. Burke, M. Ernzerhof, *Phys. Rev. Lett.* **1996**, *77*, 3865-3868.
- [68] E. van Lenthe, E. J. Baerends, *J. Comput. Chem.* **2003**, *24*, 1142-1156.
- [69] E. van Lenthe, A. Ehlers, E. J. Baerends, *J. Chem. Phys.* **1999**, *110*, 8943-8953.
- [70] E. van Lenthe, J. G. Snijders, E. J. Baerends, *J. Chem. Phys.* **1996**, *105*, 6505-6516.
- [71] E. van Lenthe, R. van Leeuwen, E. J. Baerends, J. G. Snijders, *Int. J. Quantum Chem.* **1996**, *57*, 281-293.
- [72] E. van Lenthe, E. J. Baerends, J. G. Snijders, *J. Chem. Phys.* **1994**, *101*, 9783-9792.
- [73] E. van Lenthe, E. J. Baerends, J. G. Snijders, *J. Chem. Phys.* **1993**, *99*, 4597-4610.
- [74] R. A. Kendall, T. H. Dunning Jr., R. J. Harrison, *J. Chem. Phys.* **1992**, *96*, 6796-6806.
- [75] T. H. Dunning Jr., *J. Chem. Phys.* **1989**, *90*, 1007-1023.
- [76] J. F. Stanton, J. Gauss, M. E. Harding, P. G. Szalay, *CFOUR 1.2 ed.*, Austin, TX, USA; Mainz, Germany, **2010**.
- [77] M. E. Harding, T. Metzroth, J. Gauss, *J. Chem. Theory Comput.* **2008**, *4*, 64-74.
- [78] C. C. Pye, T. Ziegler, *Theor. Chem. Acc.* **1999**, *101*, 396-408.
- [79] A. Klamt, *J. Phys. Chem.* **1996**, *100*, 3349-3353.
- [80] A. Klamt, G. Schuurmann, *J. Chem. Soc., Perkin Trans. 2* **1993**, 799-805.
- [81] R. Ditchfield, *Mol. Phys.* **1974**, *27*, 789-807.

Entry for the Table of Contents



The incarceration of *o*-benzyne and 27 other guest molecules within hemicarcerand **1** has been studied by computational NMR spectroscopy using density functional theory (DFT). The calculated $^1\text{H-NMR}$ chemical shifts showed intriguing correlations with the experimentally observed signals, providing a new strategy to characterize these challenging host-guest complexes.

Institute and/or researcher Twitter usernames:

Abril Castro: @Abril_C_Castro
Adrian Romero: @romero_adria
Silvia Osuna: @silviaosu
K. Houk: @houk1000
Marcel Swart: @Marcel_Swart